Adiabatic freezing of long-range quantum correlations in spin chains

Himadri Shekhar Dhar, Debraj Rakshit, Aditi Sen(De), and Ujjwal Sen
Harish-Chandra Research Institute, Chhatnag Road, Jhunsi, Allahabad 211 019, India

We consider a process to create quasi long-range quantum discord between the non-interacting end spins of a quantum spin chain, with the end spins weakly coupled to the bulk of the chain. The process is not only capable of creating long-range quantum correlation but the latter remains frozen, when certain weak end-couplings are adiabatically varied below certain thresholds. We term this phenomenon as adiabatic freezing of quantum correlation. We observe that the freezing is robust to moderate thermal fluctuations and is intrinsically related to the cooperative properties of the quantum spin chain. In particular, we find that the energy gap of the system remains frozen for these adiabatic variations, and moreover, considering the end spins as probes, we show that the interval of freezing can detect the anisotropy transition in quantum *XY* spin chains. Importantly, the adiabatic freezing of long-range quantum correlations can be simulated with contemporary experimental techniques.

I. INTRODUCTION

Quantum correlation [1, 2] is one of the principal characteristics that separates the quantum domain from its classical counterpart. The properties and phenomena that arise from it are neither reproducible nor simulatable in classical systems. The amount of quantum correlation that exists between two subsystems of a pure quantum state is completely captured by entanglement [1]. However, for mixed states, local measurements may reveal nonclassical features, that are present even in non-entangled or separable states [2]. Measures that capture quantum correlations beyond entanglement, such as quantum discord (QD) [3], have been instrumental in investigating several protocols of quantum information and computation (QIC) [4–6], quantum phase transitions [7], many-body dynamics [8, 9], quantum biology [10], and metrology [11, 12] (see [2], for a review).

Methods to create long-range entanglement have attracted a lot of attention due to their importance in several protocols in QIC [13–20]. Such investigations led to the discovery of processes like entanglement swapping [13] and repeaters [14], and concepts like localizable entanglement [15]. In the last decade, there have been several instances where quantum correlation measures such as QD were claimed to be important [2, 4–12]. For example, it provides an interesting perspective on the dynamics of open quantum systems [21], where entanglement is fragile. In quantum systems subject to noisy environments, for both Markovian and non-Markovian evolution, QD is more robust than entanglement [22, 23]. Interestingly, for certain types of quantum states under dephasing, QD exhibits a qualitatively different robustness. It remains *frozen* for finite evolution times [24], even though entanglement suffers sudden death. In recent times, a significant amount of research has been undertaken to characterize the phenomena of freezing of quantum correlations [25–27], including entanglement [28].

In this letter, we report quasi long-range QD between the end spins of a finite quantum spin chain, when the end spins are weakly coupled to the bulk of the spins. The work is motivated by the desire to investigate the quantum correlation properties of the end spins due to the collective effect of the bulk spins that act as a reservoir for the end spins, thus giving rise to interesting long-range quantum phenomena. In particular, we find that the long-range QD of the ground state can exhibit non-temporal freezing, while the weak end-couplings are varied. We term the freezing as "adiabatic", as the phenomenon is observed while the weak end-couplings are adiabatically varied. No such freezing behavior is observed for the long-range entanglement. The observed phenomena makes long-range QD a robust resource, against moderate thermal fluctuations and variations in certain system parameters, for implementing quantum protocols between distant spin qubits.

Interestingly, and in contradistinction to temporal freezing [24–27], the observed adiabatic phenomenon is characteristic of the quantum system rather than an external environment, and is intrinsically related to the many-body properties of the quantum spin chain. For instance, in an experimental setting, one may consider the two end-spins to be *probe* sites weakly coupled to a *system* consisting of a spin chain [17–19], where the weak end-couplings can be controlled. The long-range QD between the probe spins can then be shown to identify the nature of interaction in the system. Specifically, the freezing interval of long-range QD can be used to define an order parameter that detects the "anisotropy transition" in the system considered. Further, one can show that the adiabatic freezing phenomena is not limited to long-range quantum correlations but is also manifested in other cooperative properties of the quantum spin chain, such as the energy gap.

We note that there are recent experimental proposals and techniques to generate and characterize long-range quantum correlation in quantum spin systems [29–31] (also see Refs. [32]). In this light, we investigate the effect of thermal fluctuations in the spin system, which is important for potential experimental implementations, and find that the adiabatic freezing is stable below a critical temperature. Hence, our results show that in an experimentally accessible regime of weak end-couplings and low-temperature, high quasi-long range quantum correlations can be adiabatically frozen for applications in various quantum information protocols.

II. METHODOLOGY

Let us consider an anistropic *XY* quantum spin chain containing N spins with a closed end. The Hamiltonian for such

a system can be written as

$$\mathcal{H} = \sum_{i}^{N} \frac{\kappa}{4} \left(\mathcal{J}_i \, \sigma_i^x \sigma_{i+1}^x + \mathcal{K}_i \, \sigma_i^y \sigma_{i+1}^y\right), \tag{1}$$

where $\sigma_{N+1}^{x(y)} = \sigma_1^{x(y)}$. $\mathcal{J}_i$ and $\mathcal{K}_i$ are the dimensionless interaction strengths. $\kappa(>0)$ has the unit of energy. $\sigma^i, i = x, y, z$, are the Pauli spin matrices. The open-end case is obtained by setting $\mathcal{J}_N$ and $\mathcal{K}_N$ equal to zero.

The quantum correlation between two arbitrary sites, in the ground and thermal equilibrium state of the Hamiltonian can be obtained by deriving the two-site reduced density matrix, following the seminal work in [33]. The symmetry of the Hamiltonian ensures that all (single-site) magnetizations $\langle\sigma_i^\alpha\rangle$, $\forall\ \alpha = (x, y, z)$ vanish in the absence of any external fields. The only non-vanishing two-site terms are $\langle\sigma_i^x\sigma_j^x\rangle$, $\langle\sigma_i^y\sigma_j^y\rangle$, and $\langle\sigma_i^z\sigma_j^z\rangle$. Hence, any two-site reduced density matrix, for arbitrary sites i and j, can be written as $\rho_{ij} = 1/4(\mathbb{I} + \sum_{\alpha=x,y,z} T_{ij}^{\alpha\alpha}\ \sigma_i^\alpha \otimes \sigma_j^\alpha)$, where $T_{ij}^{\alpha\alpha} = \langle\sigma_i^\alpha\sigma_j^\alpha\rangle$ are the two-site correlation functions and $\mathbb{I}$ is the two-qubit identity matrix. $T_{ij}^{\alpha\alpha}$ can be analytically derived by solving the Hamiltonian in Eq. (1) [33, 34].

Since ρ_{ij} is Bell-diagonal, its QD [3] can be analytically obtained [35]. The eigenvalues of ρ_{ij}, in terms of $T_{ij}^{\alpha\alpha}$, is given by $\{e_i\}$ equal to $1/4(1 \pm (T_{ij}^{xx} + T_{ij}^{yy}) - T_{ij}^{zz})$ and $1/4(1 \pm (T_{ij}^{xx} - T_{ij}^{yy}) + T_{ij}^{zz})$, for i = 1 to 4. The quantum mutual information is given by the relation, $\mathcal{I}(\rho_{ij}) = \sum_i e_i \log_2(4e_i)$, and the classical correlation, obtained after optimization over measurements on a single-party, is given by $\mathcal{C}(\rho_{ij}) = \sum_{k=1}^{2} x_k \log_2(2x_k)$, where $x_k = (1 + (-1)^k\ x)/2$ (k = 1,2), and $x = \max\{|T_{ij}^{xx}|, |T_{ij}^{yy}|, |T_{ij}^{zz}|\}$. The QD is then given by the relation, $\mathcal{D}(\rho_{ij}) = \mathcal{I}(\rho_{ij}) - \mathcal{C}(\rho_{ij}) = \sum_{i=1}^{4} e_i \log_2(4e_i) - \sum_{k=1}^{2} x_k \log_2(2x_k)$. Similarly, the entanglement, using concurrence [36], between any two sites can be analytically derived in terms of the correlation function $T_{ij}^{\alpha\alpha}$ [34]: $\mathcal{E}(\rho_{ij}) = \max\left[0, 2\max[\{e_i\}] - 1\right]$.

III. ADIABATIC FREEZING OF QUANTUM DISCORD

Let us consider an N-spin non-periodic quantum spin chain, with nearest neighbor interactions, where the two spins at the edge of the chain (end spins) are weakly coupled to the remaining bulk of $N-2$ spins. The Hamiltonian for the spin is given by $\mathcal{H} = (\kappa/4)\ (\mathcal{H}_{bulk} + \mathcal{H}_{end})$, where

$$\mathcal{H}_{bulk} = \textstyle\sum_{i=2}^{N-2}(\mathcal{J}_i\ \sigma_i^x\sigma_{i+1}^x + \mathcal{K}_i\ \sigma_i^y\sigma_{i+1}^y), \tag{2}$$

$$\mathcal{H}_{end} = \lambda_1(\sigma_1^x\sigma_2^x + \sigma_{N-1}^x\sigma_N^x) + \lambda_2(\sigma_1^y\sigma_2^y + \sigma_{N-1}^y\sigma_N^y) \tag{3}$$

The above Hamiltonian can be exactly solved to calculate the quantum correlation between any two spins in the chain. The cases for which $\lambda_1 = \lambda_2 \leq \mathcal{J}_i, \mathcal{K}_i, \forall i = 2, ..., N-2$, will be referred to as "balanced" weak-coupling. It is known that for $\lambda_1(=\lambda_2) \to 0$, the two end spins in the ground state of the chain are maximally entangled. Denoting concurrence [36] by $\mathcal{E}_L$, we have $\mathcal{E}_L \to 1$ in that limit. This gives rise to quasi long-range entanglement, interestingly, in a quantum system with very short-range interaction [16, 17]. In the balanced case, $\mathcal{E}_L$ decreases monotonically with increasing $\lambda_1(=\lambda_2)$, and the rate of decay increases with system size. Also, $\mathcal{E}_L$ may exhibit non-temporal sudden death (cf. [9]).

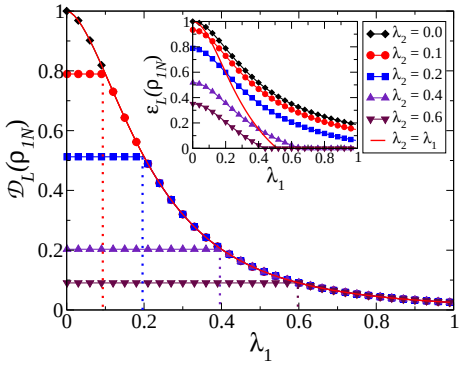

FIG. 1. (Color online.) Adiabatic freezing of quasi long-range quantum discord ($\mathcal{D}_L$). The bulk is an *XX* spin chain. For each non-zero value of λ_2, freezing of $\mathcal{D}_L$ takes place for adiabatic change of λ_1. The behavior of entanglement is given in the inset. All quantities are dimensionless, except QD (in bits) and entanglement (in ebits). Here, $N = 10$.

Let us now consider the case where $\mathcal{H}_{bulk}$ represents an ordered, *XX* spin chain, such that $\mathcal{J}_i = \mathcal{K}_i = 1, \forall\ i = 2, ..., N-2$, and the coupling strengths at the ends are such that $\lambda_1, \lambda_2 < \mathcal{J}_i$. When $\lambda_1 \neq \lambda_2$, we refer to it as "unbalanced" weak-coupling. Under such coupling, the behavior of $\mathcal{E}_L$ and long-range QD ($\mathcal{D}_L$) i.e., the QD of the reduced density matrix of the end spins, ρ_{1N}, of the ground state, are qualitatively different. Specifically, for fixed values of λ_2 and on slowly increasing the parameter λ_1, from approximately 0 to 1, $\mathcal{D}_L$ freezes, i.e., remains unchanged in value for the range $0 < \lambda_1 \leq \lambda_2$. The value of the frozen $\mathcal{D}_L$ ($\mathcal{D}_L^f$) is dependent on the fixed λ_2 and the size of the spin chain, N. However, the freezing interval (l_f), i.e., the region on the λ_1-axis over which $\mathcal{D}_L$ remains frozen, is equal to λ_2. As λ_1 is increased beyond λ_2, i.e., for the range $\lambda_1 > \lambda_2$, the freezing of $\mathcal{D}_L$ ceases and it decays exactly similar to the balanced case. Interestingly, the behavior of entanglement does not distinguish the regimes $0 < \lambda_1 \leq \lambda_2$ and $\lambda_1 > \lambda_2$. In particular, $\mathcal{E}_L$ decays in a similar fashion in both the regimes, though the maximum $\mathcal{E}_L$ at $\lambda_1 \approx 0$ and the value of λ_1 at the non-temporal death (i.e., λ_1^D, such that for all $\lambda_1 \geq \lambda_1^D, \mathcal{E}_L = 0$), both decrease with increasing λ_2. Figure 1 shows the freezing of long-range QD in an $N = 10$ spin *XX* chain for different values of the fixed weak coupling, λ_2, with the variation of λ_1. We call such phenomenon as "adiabatic freezing" since it can be observed in the adiabatic evolution obtained by slow variation of the weak coupling λ_1. The phenomenon of adiabatic freezing can be explained by observing the behavior of the two-site correlation functions that are obtained by solving the Hamiltonian in Eq. (3). Note that the freezing of $\mathcal{D}_L$ observed in the present context is purely a property of the quantum spin chain, and not a conjunction of the system and an environment.

We note that both $\mathcal{E}_L$ and $\mathcal{D}_L$ are quasi long-range [17], i.e.,

their value decreases with increase in system-size N. Hence, for a fixed λ_2, the frozen discord value, $\mathcal{D}_L^f$, decreases as N grows larger. However, fixing the weak-end couplings to low values, say $\lambda_1/\mathcal{J}_i \approx 0.001$, for N=200, a reasonably high $\mathcal{D}_L^f \approx 0.93$ can be obtained, and frozen upto one order higher, i.e., $l_f = \lambda_2 = 0.01$. Moreover, even symmetric quantum correlation measures, such as symmetric QD [37], exhibits adiabatic freezing for $\lambda_1 \neq \lambda_2$.

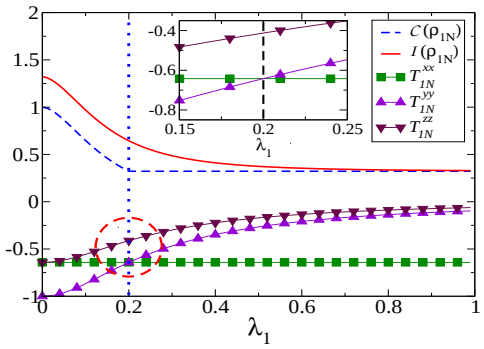

FIG. 2. (Color online.) Variation of $\mathcal{I}(\rho_{1N})$, $\mathcal{C}(\rho_{1N})$, and $T^{\alpha\alpha}_{1N}$ with increase in the end coupling λ_1, for a fixed $\lambda_2 = 0.2$, and for N = 20 spins, where the bulk is an *XX* chain. $\mathcal{D}_L$ is frozen for $\lambda_1 \leq \lambda_2$. $\mathcal{D}_L^f$ = 0.322 and l_f = 0.2. All quantities used are dimensionless except $\mathcal{D}_L$, $\mathcal{I}(\rho_{1N})$, and $\mathcal{C}(\rho_{1N})$, which are in bits. The inset magnifies the red-encircled region.

The analysis of two-site correlation functions between the end spins, $T^{\alpha\alpha}_{1N}$, can shed light on the observed adiabatic freezing of QD. From Fig. 2, for N = 20 spins with λ_2 = 0.2, we observe that $T^{\alpha\alpha}_{1N} < 0$, and $|T^{\alpha\alpha}_{1N}| < 1$, $\forall\ \alpha$. Since, $T^{zz}_{1N} = -\,T^{xx}_{1N}\,T^{yy}_{1N}$ [33, 34], therefore T^{xx}_{1N} and T^{yy}_{1N} are the only independent variables, with $|T^{zz}_{1N}| \leq |T^{xx}_{1N}|$ and $|T^{zz}_{1N}| \leq |T^{yy}_{1N}|$. Moreover, it is seen that T^{xx}_{1N} is constant during the adiabatic evolution. Hence, the quantum mutual information ($\mathcal{I}(\rho_{1N})$) is an entropic function of $1 \pm T^{yy}_{1N}$. Since, $|T^{yy}_{1N}| \geq |T^{xx}_{1N}| \geq |T^{zz}_{1N}|$ for $\lambda_1 \leq \lambda_2$, the classical correlation ($\mathcal{C}(\rho_{1N})$) is also a function of $1 \pm T^{yy}_{1N}$. Hence, $\mathcal{I}(\rho_{1N})$ and $\mathcal{C}(\rho_{1N})$ decay with identical rates leading to a constant long-range QD. However, for $\lambda_1 > \lambda_2$, $|T^{xx}_{1N}| > |T^{yy}_{1N}| \geq |T^{zz}_{1N}|$ and $\mathcal{C}(\rho_{1N})$ is now a function of $1 \pm T^{xx}_{1N}$. Since, T^{xx}_{1N} is constant during the evolution, $\mathcal{C}(\rho_{1N})$ freezes for $\lambda_1 > \lambda_2$, in contrast to $\mathcal{I}(\rho_{1N})$ in that range. Hence, the freezing of the long-range $\mathcal{D}_L(\rho_{1N})$ disappears for $\lambda_1 > \lambda_2$. As $\lambda_2 \to \{0, \lambda_1\}$, there is no freezing of $\mathcal{D}_L(\rho_{1N})$, as $\mathcal{C}(\rho_{1N})$ is always constant. In contrast, for entanglement, no adiabatic freezing occurs. In Fig. 2, since $0 < |T^{\alpha\alpha}_{1N}| < 1$, $\forall\ \alpha$, $\mathcal{E}_L$ is given by the relation, $\mathcal{E}_L = \max[0, 1/2(g_{1N} - h_{1N})]$, where, $g_{1N} = |T^{xx}_{1N} + T^{yy}_{1N}|$, and $h_{1N} = 1 - |T^{xx}_{1N}||T^{yy}_{1N}| > 0$. As λ_1 increases g_{1N} and h_{1N} decreases, due to decreasing $|T^{yy}_{1N}|$, and constant $|T^{xx}_{1N}|$. For $g_{1N} > h_{1N}$, $\mathcal{E}_L$ decreases with λ_1, and at $g_{1N} \leq h_{1N}$, $\mathcal{E}_L$ = 0 (sudden death). For $\lambda_1 = \lambda_2$, we have $T^{xx}_{1N} = T^{yy}_{1N} = z$ (say). Therefore, $\mathcal{E}_L = \max\left[0, 1/2(z^2 + 2|z| - 1))\right]$ [34].

The observed behavior of $\mathcal{I}(\rho_{1N})$ and $\mathcal{C}(\rho_{1N})$ is consistent to what is observed in the freezing of QD, first observed in dephasing quantum systems [24], that heralded a substantial amount of research in recent years [25–27]. However, we note that the freezing of $\mathcal{D}_L(\rho_{1N})$ observed in the present context is purely a property of the long-range correlations in the spin chain and is devoid of any external decoherence, in contrast to conventional freezing phenomena.

IV. DETECTING ANISOTROPY TRANSITION

The adiabatic freezing of the quasi long-range QD ($\mathcal{D}_L$) in spin chains, with Hamiltonians of the form given by Eq. (3), can be used to investigate certain intrinsic properties of the bulk Hamiltonian, such as the anisotropy transition. Though there exist methods to detect anisotropy in quantum spin systems [38], our results provide an information-theoretic perspective to investigate these quantum properties in an experimentally viable manner.

Let $\mathcal{H}_{bulk}$ be an ordered *XY* spin chain with $\mathcal{J}_i = 1 + \gamma$ and $\mathcal{K}_i = 1 - \gamma$, $\forall\ i = 2, ..., N-2$, with $\gamma(\neq 0)$ being the finite anisotropy present in $\mathcal{H}_{bulk}$. The end-coupling is unbalanced, such that $\lambda_1 \neq \lambda_2$. We focus on the parameter regime $\lambda_1, \lambda_2 \leq 1$, where the relevant physics under consideration is clearly observed. Let us now consider the adiabatic freezing of $\mathcal{D}_L$ in the above spin chain, with possible anisotropy in $\mathcal{H}_{bulk}$, by varying the weak end-couplings. The presence of anisotropy introduces changes in the freezing characteristics of $\mathcal{D}_L$. For instance, $\mathcal{D}_L^f$ increases with γ upto a certain fixed value that depends on N, and then decreases. See inset of Fig. 3. Interestingly, the freezing interval, l_f undergoes a transition that can detect the anisotropy transition at $\gamma = 0$ in the bulk spin system. This allows us to define an anisotropy transition order in terms of the system parameters and the freezing interval l_f. This can be seen as follows. We evaluate l_f for different values of λ_1, and a fixed λ_2. By using $\lambda_2 - l_f$ as the order parameter, one can detect the γ–transition in the system at $\gamma = 0$, driven by changes in the anisotropy parameter.

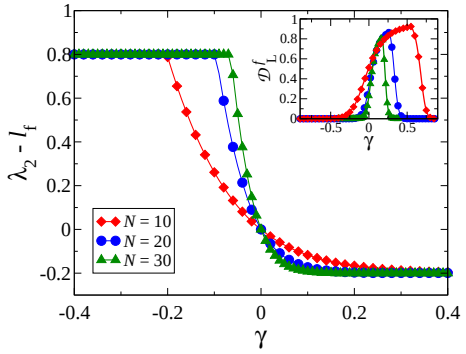

FIG. 3. (Color online.) Detecting the anisotropy (γ) transition. The order parameter, $\lambda_2 - l_f$ is plotted against γ, with fixed λ_2. The inset shows that $\mathcal{D}_L^f$ can be substantially increased for positive γ, below a threshold value. The anisotropy transition can also be seen from the change in the curvature (convexity to concavity) of $\mathcal{D}_L^f$ with respect to γ, where the N-dependent critical values approach $\gamma = 0$ through negative γ. All quantities are dimensionless, except QD (in bits).

The order parameter $\lambda_2 - l_f$ is finite for anisotropic systems and vanishes at $\gamma = 0$. Further, one observes that $\lambda_2 - l_f$ sharply decreases as γ is increased beyond an N-dependent threshold value (γ_c^N). It is observed that as N is increased upto certain values, the critical parameter $\gamma_c^N \to 0$. Hence, for large but finite N, transition in $\lambda_2 - l_f$ at γ_c^N captures the γ–transition of the class of quantum spin models described by the Hamiltonian in Eq. (3). The observed transition is shown and described in Fig. 3.

In an experimental setting, one may consider the end spins to be probe sites at the edge of a quantum spin chain consisting of the bulk spins. The two end-spins can be defects or scattering particles in a spin chain [17, 39], and the weak end-coupling can be experimentally controlled. Under such conditions, the anisotropy of $\mathcal{H}_{bulk}$ can be detected using the order parameter $\lambda_2 - l_f$, where the desired quantities are observed from the freezing of long-range QD between the two probe spins. Hence, the quantity $\lambda_2 - l_f$ can serve as a suitable order parameter in many-body simulations. The advantage of the approach lies in the fact that all performed measurements and tuning of interactions are associated only with the probe spins that weakly interact with the quantum spin chain. The detection of the intrinsic anisotropy in the bulk spin chain is achieved without disturbing the system. This provides an interesting role for adiabatic freezing of discord in investigating many-body phenomena.

V. FREEZING OF ENERGY GAP

Another interesting phenomenon that connects adiabatic freezing of long-range quantum correlations to the cooperative properties of the quantum spin chain, is the freezing of energy gap. For the considered model, the weak end-couplings between the bulk and end spins introduces a finite energy gap.

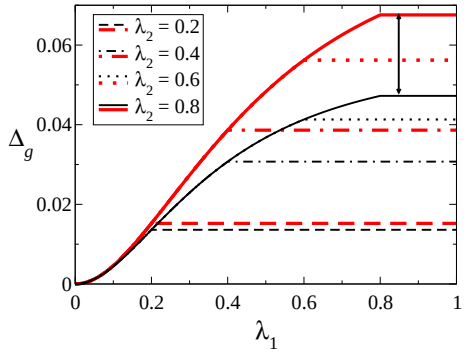

FIG. 4. (Color online.) Adiabatic freezing of the energy gap. Numerically obtained values of Δ_g is plotted against λ_1, for different fixed values of λ_2. The spin model is the same as in Fig. 1, but for $N = 20$ (red) and 30 (black). For $\lambda_1 \geq \lambda_2$, Δ_g is frozen. The difference in frozen Δ_g for different N, marked in one case with a double-headed arrow, increases with λ_2. All quantities plotted are dimensionless. Note that the behavior of Δ_g and $\mathcal{D}_L$ with response to λ_1, for fixed λ_2, is complementary.

The energy gap is an intrinsic property of a quantum spin system that can be obtained from the excitation energy spectrum or the dispersion relation of the function Δ_k [33, 34]. Let us consider the system, where $\mathcal{H}_{bulk}$ in Eq. (2), represents an ordered *XX* spin chain. The only anisotropy in the system arises from the coupling strengths at the end spins. Solving the Hamiltonian, one can obtain the excitation spectrum, Δ_k.

For the balanced case, $\lambda_1 = \lambda_2 = \lambda$, the dispersion relation of the excitation energy is given by $\Delta_k = \cos(k)$, where k are the quasimomenta modes. These modes satisfy the eigenvalue equation [16], $\mu \cot(k)[\cot((N-1)k/2)]^\mu = \lambda^2/(2-\lambda^2)$, for $\lambda \neq 1$, with $\mu = \pm 1$ being the eigenstate parity. Considering $\mu = 1$, the energy gap is then given by k', which minimizes $\Delta_{k'} = \cos(k')$, while satisfying the above eigenvalue equation. For $N \gg 1$, at $k' = \pi/2 - \delta$, where $\delta \to 0$, an analytical expression for the energy gap (Δ_g) is obtained [17], where $\Delta_g \approx (\pi/2N)[(1 + 2/(N(\lambda^2/(2-\lambda^2)+2)] = f(\lambda)$. Numerical analysis shows that for the case, $\lambda_1 \neq \lambda_2$, the quasimomenta k' corresponding to the energy gap satisfies the eigenvalue equation for $\lambda = \min[\lambda_1, \lambda_2]$. Therefore, the energy gap is given by the relation, $\Delta_g = \min[f(\lambda_1), f(\lambda_2)]$, where $f(\lambda)$, defined above, is a monotonically decreasing function of λ. The adiabatic freezing of the numerically estimated energy gap, is shown in Fig. 4. Using the above relation for Δ_g and monotonicity of the function $f(\lambda)$, it is obvious that Δ_g freezes for $\lambda_2 \leq \lambda_1$, since in this region, $f(\lambda_2) \leq f(\lambda_1)$ and Δ_g is thus independent of λ_1.

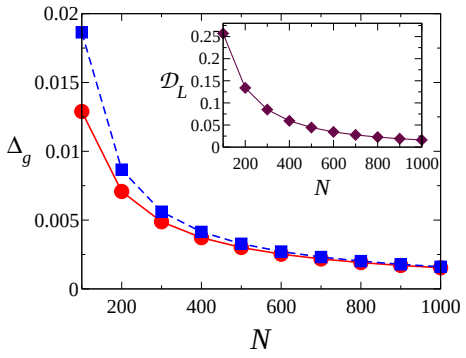

FIG. 5. (Color online.) Variation of the analytically and numerically estimated values of the energy gap with increasing size of the spin chain. The analytical expression is given by $\Delta_g = \min[f(\lambda_1), f(\lambda_2)]$ (blue-square), and is observed to be consistent with numerically obtained values of Δ_g (red-circle) at large N, for $\lambda_1 = 0.4$ and $\lambda_2 = 0.6$ (and, $\lambda_1 = 0.6$ and $\lambda_2 = 0.4$). The inset shows $\mathcal{D}_L$ (maroon-diamonds) with increasing N. The figure shows that at large N, Δ_g and $\mathcal{D}_L$ scale as $1/N$.

The adiabatic freezing of Δ_g is complementary to that of $\mathcal{D}_L$, in terms of the variation of weak end-couplings. Figs. 1 and 4 show that while $\mathcal{D}_L$ freezes for $\lambda_1 \leq \lambda_2$, Δ_g is constant for $\lambda_1 \geq \lambda_2$. Moreover, while the frozen value of $\mathcal{D}_L$ decreases with increase in λ_2, it does the opposite for Δ_g. Figure 5 shows the agreement between the analytically and numerically obtained values of Δ_g, at large N. We observe that at large N, the frozen values of both Δ_g and $\mathcal{D}_L$ scale with $1/N$ [34]. The behavior of Δ_g shows that the phenomenon of adiabatic freezing is manifested through the intrinsic proper-

ties of the quantum spin chain.

VI. RESPONSE TO THERMAL FLUCTUATIONS

In the previous sections, the phenomena of freezing is observed for the ground state of the quantum spin chain under consideration. For small thermal fluctuations, the system is no longer in the ground-state, but a mixed state in equilibrium at some small temperature (T). To obtain the reduced two-site density matrix of the thermal equilibrium state of the spin system, at temperature T, one must find the thermal two-site correlation functions $T_{ij}^{\alpha\alpha}(\beta)$ [33, 34]. Here, $\beta = 1/k_B T$, where k_B is the Boltzmann constant.

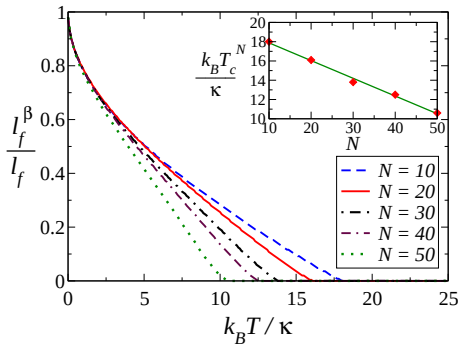

FIG. 6. (Color online.) Response of freezing to thermal fluctuations. We plot the ratio of the thermal freezing interval (l_f^β) and the ground state freezing interval (l_f) as a function of temperature. Here, λ_2= 0.2. We observe that for every N, there exists a critical temperature (T_c^N) beyond which adiabatic freezing disappears for finite chains. T_c^N decreases linearly with N, as shown in the inset. The solid green line, in the inset, is the linear fit, $y = 19.72 - 0.184x$. All quantities plotted are dimensionless.The abscissae in the figure and the ordinates in the inset are multiplied by 10^4.

We observe that adiabatic freezing persists at finite T, below a critical temperature T_c^N, that also depends on the system-size N. The value of frozen discord $\mathcal{D}_L^f$ is constant for temperatures below T_c^N, though the freezing interval decreases as T increases. T_c^N is a linearly decreasing function of N. Figure 6 shows the effect of thermal excitations on freezing interval of long-range QD in an *XX* spin chain.

VII. DISCUSSION

In recent years, experimental generation of long-range quantum correlation in antiferromagnetic spins chains have been reported using strontium-cuprate compounds, such as $Sr_{14}Cu_{24}O_{41}$, to simulate dimerized spin-chains [29]. Quantum correlations are experimentally measured using low temperature magnetization, magnetic susceptibility, and heat capacity [29, 32]. Another experimental protocol, relevant to the quantum spin chain considered in our study, was proposed using ions of the ytterbium isotope, ^{171}Yb, in segmented linear Paul traps [30], utilizing the tailoring of axial trapping potential to generate the spin-spin coupling, and using microwave pulses to generate effective spin interactions. A more recent study devises a similar scheme using superconducting flux qubits, using dc currents and microwave pulses to control the spin-spin interaction [31]. Moreover, recent experimental studies have also observed the freezing phenomena in various quantum systems [25].

In our work, we find that there exists adiabatic freezing of quasi long-range quantum correlations in finite quantum spin chains. We show that the observed phenomena is robust to the weak end-spin couplings and finite thermal fluctuations, which are the fundamental elements in experimental control of quantum systems. Further, by tuning the end-spin coupling one can obtain relatively high values of long-range QD. Interestingly, we have observed that a finite interaction between the two end spins can vastly increase the shared QD between the sites, without affecting the freezing interval. This is intuitively plausible, as the finite end-to-end coupling encourages greater correlation between the end spins. Alternatively, one can also study the phenomena in the *XX* and *XY* spin chains in a transverse magnetic field. Preliminary investigations reveal that, for weak end-couplings, an effective freezing [27] of long-range QD can be characterized. For quantum spin chains such as the frustrated spin-1/2 $J_1 - J_2$ model, spin-1/2 *XX* chain with alternating interactions, and the spin-1 AKLT model, long-range quantum correlations are observed [17], although adiabatic freezing is absent. We also note that the phenomenon of adiabatic freezing can be utilized to experimentally detect properties of quantum spin-baths, modelled by an interacting bulk spin Hamiltonian, and probed by weakly interacting spins at ends of the bath.

To conclude, we find the phenomenon of adiabatic freezing of quasi long-range QD in the closed dynamics of many-body quantum systems. Our work makes a connection between the temporal freezing of correlations, observed only in damped quantum systems, to the feature of long-range correlations in quantum spin chains. However, in contrast to temporal freezing, the adiabatic phenomena is an intrinsic property of the considered spin system. It has the ability to detect important cooperative phenomena in quantum spin models and in particular serve as an order parameter for detecting the anisotropy transition in quantum XY models. We note that the phenomena is also observed for other system properties such as energy gap, and other quantum correlation measures such as symmetric discord [37] and one-way quantum work-deficit [40].

With unprecedented developments to simulate quantum spin chains in different physical substrates and experimental techniques to characterize quantum correlations, the phenomenon of adiabatic freezing allows the generation of robust long-range quantum correlations between distant parties, for application in future quantum technologies.

[1] Horodecki R., Horodecki P., Horodecki M. and Horodecki K., *Rev. Mod. Phys.*, **81** (2009) 865.

[2] Modi K., Brodutch A., Cable H., Paterek T. and Vedral V., *Rev. Mod. Phys.*, **84** (2012) 1655.

[3] Henderson L. and Vedral V., *J. Phys. A*, **34** (2001) 6899; Ollivier H. and Zurek W. H. , *Phys. Rev. Lett.*, **88** (2002) 017901.

[4] Datta A., Shaji A. and Caves C. M., *Phys. Rev. Lett.*, **100** (2008) 050502; Lanyon B. P., Barbieri M., Almeida M. P., and White A. G., *Phys. Rev. Lett.*, **101**, (2008) 200501.

[5] Madhok V. and Datta A., *Phys. Rev. A*, **83** (2011) 032323; Cavalcanti D., Aolita L., Boixo S., Modi K., Piani M. and Winter A., *Phys. Rev. A*, **83** (2011) 032324; Pirandola S., *Sci. Rep.*, **4** (2014) 6956.

[6] Dakić B. *et al.*, *Nat. Phys.*, **8** (2012) 666; Gu M. *et al.*, *Nat. Phys.*, **8** (2012) 671.

[7] Dillenschneider R., *Phys. Rev. B*, **78** (2008) 224413; Sarandy M. S., *Phys. Rev. A*, **80** (2009) 022108; Werlang T., Ribeiro G. A. P. and Rigolin G., *Phys. Rev. Lett.*, **83** (2011) 062334; Liu B. -Q., Shao B., Li J.-G., Zou J. and Wu L.-A., *Phys. Rev. A*, **83** (2011) 052112; Allegra M., Giorda P. and Montorsi A., *Phys. Rev. B*, **84** (2011) 245133.

[8] Werlang T. and Rigolin G., *Phys. Rev. A*, **81** (2011) 044101; Campbell S. *et al.*, *Phys. Rev. A*, **84** (2011) 052316; Mazzola L. and Paternostro M., *Sci. Rep.*, **1** (2011) 199; Tomasello B., Rossini D., Hamma A. and Amico L., *EPL*, **96** (2011) 27002; Amico L., Rossini D., Hamma A. and Korepin V. E., *Phys. Rev. Lett.*, **108** (2012) 240503; Prabhu R., Sen(De) A. and Sen U., *Phys. Rev. A*, **86** (2012) 012336; Maziero J., Céleri L. C., Serra R. M. and Sarandy M. S., *Phys. Lett. A*, **376** (2012) 1540; Pal A. K. and Bose I., *Eur. Phys. J. B*, **85** (2012) 36; *Eur. Phys. J. B*, **85** (2012) 277; Mishra U., Prabhu R., Sen(De) A. and Sen U., *Phys. Rev. A*, **87** (2013) 052318; Ciliberti L., Canosa N., and Rossignoli R. *Phys. Rev. A*, **88** (2013) 012119; Cianciaruso M. *et al.*, arXiv:1412.1054; Huang Y., *Phys. Rev. B*, **89** (2014) 054410.

[9] Dhar H. S., Ghosh R., Sen(De) A. and Sen U, *EPL*, **98** (2012) 30013; *Phys. Lett. A*, **378** (2014) 1258.

[10] Brádler K., Wilde M. M., Vinjanampathy S. and Uskov D. B., *Phys. Rev. A*, **82** (2010) 062310; Chanda T., Mishra U., Sen(De) A. and Sen U., arXiv:1412.6519.

[11] Modi K., Cable H., Williamson M. and Vedral V., *Phys. Rev. X*, **1** (2011) 021022.

[12] Girolami D., Tufarelli T. and Adesso G., *Phys. Rev. Lett.*, **110** (2013) 240402; Girolami D. *et al.*, *ibid.*, **112** (2014) 210401.

[13] Żukowski M., Zeilinger A., Horne M. A. and Ekert A. K., *Phys. Rev. Lett.*, **71** (1993) 4287; Żukowski M., Zeilinger A. and Weinfurter H., *Annals N.Y. Acad. Sci.*, **755** (1995) 91; Bose S., Vedral V. and Knight P. L., *Phys. Rev. A*, **57** (1998) 822.

[14] Briegel H.-J., Dür W., Cirac J. I. and Zoller P., *Phys. Rev. Lett.*, **81** (1998) 5932.

[15] Verstraete F., Popp M., and Cirac J. I., *Phys. Rev. Lett.*, **92** (2004) 027901; Popp M., Verstraete F., Martín-Delgado M. A. and Cirac J. I., *Phys. Rev. A*, **71** (2005) 042306.

[16] Wójcik A., Łuczak T., Kurzyński P., Grudka A., Gdala T. and Bednarska M., *Phys. Rev. A*, **72** (2005) 034303.

[17] Venuti L. C., Degli E. B. C. and Roncaglia M., *Phys. Rev. Lett.*, **96** (2006) 247206; *ibid.*, **99** (2007) 060401; Venuti L. C., Giampaolo S. M., Illuminati F. and Zanardi P., *Phys. Rev. A*, **76** (2007) 052328.

[18] Giampaolo S. M. and Illuminati F., *Phys. Rev. A*, **80** 050301 (2009); *New J. Phys.*, **12** (2010) 025019.

[19] Yang S., Bayat A. and Bose S., *Phys. Rev. A*, 84 (2011) 020302(R); Bayat A., Sodano P. and Bose S., *Quant. Inf. Proc.*, **11** (2012) 89.

[20] Son W., Amico L., Plastina F., and Vedral V., *Phys. Rev. A*, **79** (2009) 022302.

[21] Breuer H.-P. and Petruccione F., *The Theory of Open Quantum Systems* (Oxford University Press, Oxford) 2002.

[22] Werlang T., Souza S., Fanchini F. F. and Villas Boas C. J., *Phys. Rev. A*, **80** (2009) 024103; Lo Franco R., Bellomo B., Maniscalco S. and Compagno G. , *Int. J. Mod. Phys. B*, **27** (2013) 1345053, and references therein.

[23] Yu T. and Eberly J. H., *Phys. Rev. Lett.*, **93** (2004) 140404; Almeida M. P., de Melo F., Hor-Meyll M., Salles A., Walborn S. P., Ribeiro P. H. S. and Davidovich L., *Science*, **316** (2007) 579.

[24] Mazzola L., Piilo J. and Maniscalco S., *Phys. Rev. Lett.*, **104** (2010) 200401.

[25] Xu J.-S., Xu X.-Y., Li C.-F., Zhang C.-J., Zou X.-B. and Guo G.-C., *Nat. Comm.*, **1** (2010) 7; Auccaise R. *et al.*, *Phys. Rev. Lett.*, **107** (2011) 140403; Silva I. A. *et al.*, *Phys. Rev. Lett.*, **110** (2013) 140501.

[26] Haikka P., Johnson T. H. and Maniscalco S., *Phys. Rev. A*, **87** (2013) 010103(R); Mazzola L., Piilo J. and Maniscalco S., *Int. J. Quant. Inf.*, **09** (2011) 981; Bellomo B., Lo Franco R. and Compagno G., *Phys. Rev. A*, **86** (2012) 012312; Xu J.-S. *et al.*, *Nat. Commun.*, **4**, (2013) 2851; Montealegre J. D., Paula F.M., Saguia A. and Sarandy M. S., *Phys. Rev. A*, **87** (2013) 042115; Cianciaruso M., Bromley T. R., Roga W., Lo Franco R. and Adesso G., *Sci. Rep.*, **5**, (2015) 10177; Bromley T. R., Cianciaruso M. and Adesso G., *Phys. Rev. Lett.*, **114** (2015) 210401.

[27] Chanda T., Pal A. K., Biswas A., Sen(De) A., and Sen U., *Phys. Rev. A*, **91** (2015) 062119.

[28] Carnio E. G., Buchleitner A. and Gessner M., *Phys. Rev. Lett.*, **115** (2015) 010404.

[29] Sahling S. *et al.*, *Nat. Phys.*, **11** (2015), 255.

[30] Zippilli S., Johanning M., Giampaolo S. M., Wunderlich Ch. and Illuminati F., *Phys. Rev. A*, **89** (2014) 042308.

[31] Zippilli S., Grajcar M., Il'ichev E. and Illuminati F., *Phys. Rev. A*, **91** (2015) 022315.

[32] Aenesen M. C. Bose S. and Vedral V., *Phys. Rev. Lett.*, **87** (2001) 017901; Wiesniak M., Vedral V. and Brukner C., *New J. Phys.*, **7** (2005) 258; Lima Sharma A. L. and Gomes A. M., *EPL*, **84** (2008) 60003; Chakraborty T., Singh H., Singh S., Gopal R. K., and Mitra C., *J. Phys. Condens. Matter*, **25** (2013) 425601; Chakraborty T., Sen T. K., Singh H., Das D., Mandal S. K. and Mitra C., *J. Appl. Phys.*, **114** (2013) 144904; Chakraborty T., Singh H. and Mitra C. , *ibid.*, **115** (2014) 034909.

[33] Lieb E., Schultz T. and Mattis D., *Ann. Phys.*, **16** (1961) 407.; Barouch E., McCoy B. M. and Dresden M., *Phys. Rev. A*, **2** (1970) 1075; Barouch E. and McCoy B. M., *Phys. Rev. A*, **3** (1971) 786.

[34] See Supplementary Material at the end of the manuscript for further details.

[35] Luo S., *Phys. Rev. A*, **77** 042303 (2008).

[36] Hill S. and Wootters W. K., *Phys. Rev. Lett.*, **78** 5022 (1997); Wootters W. K., *ibid.*, **80** 2245 (1998).

[37] Rulli C. C. and Sarandy M. S., *Phys. Rev. A*, **84** 042109 (2011).

[38] Cuccoli A., Roscilde T., Vaia R., and Verrucchi P., *Phys. Rev. Lett.*, **90** 167205 (2003).

[39] Chiara G. D., Brukner C., Fazio R., Palma G. M. and Vedral V., *New J. Phys.*, **8** 95 (2006).

[40] Horodecki M. *et al.*, *Phys. Rev. A*, **71** (2005) 062307.

Supplementary Material

S1. SPIN HAMILTONIAN AND CORRELATION FUNCTIONS

Let us consider an anistropic XY quantum spin chain containing N spins with a closed end. The Hamiltonian for such a system can be written as

$$\mathcal{H} = \sum_{i}^{N} \frac{\kappa}{4} \left(\mathcal{J}_i \, \sigma_i^x \sigma_{i+1}^x + \mathcal{K}_i \, \sigma_i^y \sigma_{i+1}^y\right), \tag{s1}$$

where $\sigma_{N+1}^{x(y)} = \sigma_1^{x(y)}$. $\mathcal{J}_i$ and $\mathcal{K}_i$ are the dimensionless interaction strengths. $\kappa(>0)$ has the unit of energy. σ^i, $i = x, y, z$, are the Pauli spin matrices. The open-end case is obtained by setting $\mathcal{J}_N$ and $\mathcal{K}_N$ equal to zero.

The two-site quantum correlation, between arbitrary sites, in the ground state of the Hamiltonian can be obtained by deriving the two-site reduced density matrix, following the seminal work in [S1]. The Hamiltonian given in Eq. (s1), can be transformed in terms of spin-raising and -lowering operators, $\hat{a}_i^\dagger = \sigma_i^x + i\sigma_i^y$ and $\hat{a}_i = \sigma_i^x - i\sigma_i^y$, to obtain

$$\mathcal{H} = \frac{\kappa}{2} \sum_{i} (\mathcal{J}_i' \, \hat{a}_i^\dagger \hat{a}_{i+1} + \mathcal{K}_i' \, \hat{a}_i^\dagger \hat{a}_{i+1}^\dagger + \text{h.c.}), \tag{s2}$$

where $\mathcal{J}_i' = (\mathcal{J}_i + \mathcal{K}_i)/2$ and $\mathcal{K}_i' = (\mathcal{J}_i - \mathcal{K}_i)/2$. The partly-Fermi, partly-Bose operators ($\hat{a}^\dagger$) can be transformed to a set of strictly Fermi operators ($\hat{k}^\dagger$), using the Jordan-Wigner transformations [S2], such that $\hat{k}_i = \exp\left[i\pi \sum_{j=1}^{i-1} \hat{a}_j^\dagger \hat{a}_j\right] \hat{a}_i^\dagger$ and $\hat{k}_i^\dagger = \hat{a}_i^\dagger \exp\left[-i\pi \sum_{j=1}^{i-1} \hat{a}_j^\dagger \hat{a}_j\right]$. Equation (s1) takes a quadratic form in terms of the Fermi creation ($\hat{k}^\dagger$) and annihilation ($\hat{k}$) operators, that can be diagonalized. The quadratic-form Hamiltonian is given by $\mathcal{H} = \kappa \sum_{ij} \hat{k}_i^\dagger \mathcal{A}_{ij} \hat{k}_j + \frac{1}{2}(\hat{k}_i^\dagger \mathcal{B}_{ij} \, \hat{k}_j^\dagger + \text{h.c.})$, where $\mathcal{A}_{ij} = \frac{1}{2}(\mathcal{J}_i' \delta_{i+1,j} + \mathcal{J}_j' \delta_{i,j+1})$ is a symmetric matrix and $\mathcal{B}_{ij} = \frac{1}{2}(\mathcal{K}_i' \delta_{i+1,j} - \mathcal{K}_j' \delta_{i,j+1})$ is an anti-symmetric matrix. For closed-ended chains, $\mathcal{A}_{1N} = \mathcal{A}_{N1} = \mathcal{J}_N'$ and $\mathcal{B}_{1N} = -\mathcal{B}_{N1} = \mathcal{K}_N'$. As shown in [S1], any two-site reduced density matrix of the ground state, for arbitrary sites, can be derived in terms of the matrices $\mathcal{A}$ and $\mathcal{B}$, by solving the eigenvalue equation, $\phi_k(\mathcal{A} - \mathcal{B})(\mathcal{A} + \mathcal{B}) = \Delta_k^2 \phi_k$. The dispersion relation of the function Δ_k gives us the excitation spectrum that can be used to estimate the energy gap in the system. A corresponding vector, ψ_k, is defined as $\psi_k = \frac{1}{\Delta_k}(\mathcal{A} + \mathcal{B})\phi_k$. A unitary correlation matrix, $\mathcal{G}$ is then obtained by the relation, $\mathcal{G}_{ij} = -\sum_k \psi_{ki} \, \phi_{kj}$.

The two-site reduced density matrix can be obtained from the single-site magnetizations, $\langle \sigma_i^\alpha \rangle$, and the two-site correlation functions, $\langle \sigma_i^\alpha \sigma_j^\beta \rangle - \langle \sigma_i^\alpha \rangle \langle \sigma_j^\beta \rangle$, where $(\alpha, \beta = x, y, z)$. The symmetry of the Hamiltonian ensures that the only non-vanishing (single-site) magnetization is $\langle \sigma_i^z \rangle$. However, for no external fields, the single-site magnetization also vanishes. Moreover, the only non-vanishing two-site terms are $\langle \sigma_i^x \sigma_j^x \rangle$, $\langle \sigma_i^y \sigma_j^y \rangle$, and $\langle \sigma_i^z \sigma_j^z \rangle$, which gives us the two-site correlation functions, since $\langle \sigma_i^\alpha \rangle = 0, \forall \, \alpha$. In terms of the correlation matrix, $\mathcal{G}$, derived in the main text by diagonalizing the Hamiltonian in Eq. (s1), the correlation functions are given by [S1],

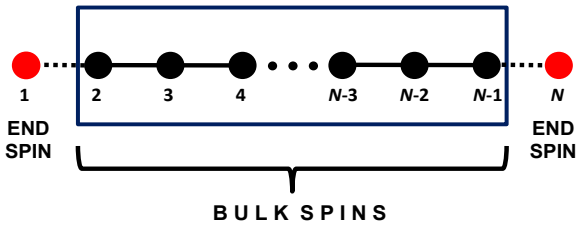

FIG. s1. (Color online.) The set-up. The end spins are weakly coupled (black-dashed lines) with the bulk, which are strongly coupled to each other (black solid line).

$$T_{ij}^{xx} = \begin{vmatrix} \mathcal{G}_{i,i+1} & .. & \mathcal{G}_{i,j} \\ \vdots & & \vdots \\ \mathcal{G}_{j-1,i+1} & .. & \mathcal{G}_{j-1,j} \end{vmatrix},$$

$$T_{ij}^{yy} = \begin{vmatrix} \mathcal{G}_{i+1,i} & .. & \mathcal{G}_{i+1,j-1} \\ \vdots & & \vdots \\ \mathcal{G}_{j,i} & .. & \mathcal{G}_{j,j-1} \end{vmatrix},$$

$$T_{ij}^{zz} = (\mathcal{G}_{i,i}\mathcal{G}_{j,j} - \mathcal{G}_{i,j}\mathcal{G}_{j,i}). \tag{s3}$$

Note that T^{xx} and T^{yy} are minors of the determinant of $\mathcal{G}$. For nearest neighbors, the above correlations reduce to $T_{i,i+1}^{xx} = \mathcal{G}_{i,i+1}$, $T_{i,i+1}^{yy} = \mathcal{G}_{i+1,i}$, and $T_{i,i+1}^{zz} = -\mathcal{G}_{i,i+1}\,\mathcal{G}_{i+1,i}$, since $\langle \sigma_i^z \rangle = -\mathcal{G}_{ii} = 0$. For the end-to-end spin (see Fig. s1), two-site correlation function, ($T_{1,N}^{\alpha\alpha}$), the minor is an $N-1 \times N-1$ matrix and the expressions in Eq. (s3) can be simplified to obtain the following:

$$\begin{aligned} T_{1,N}^{xx} &= -\mathcal{G}_{N,1} \det(\mathcal{A} - \mathcal{B})/|\det(\mathcal{A} - \mathcal{B})| = \mathcal{G}_{N,1}, \\ T_{1,N}^{yy} &= -\mathcal{G}_{1,N} \det(\mathcal{A} - \mathcal{B})/|\det(\mathcal{A} - \mathcal{B})| = \mathcal{G}_{1,N}, \text{and} \\ T_{1,N}^{zz} &= -\mathcal{G}_{1,N}\,\mathcal{G}_{N,1} = -T_{1,N}^{xx}\,T_{1,N}^{yy}. \end{aligned} \tag{s4}$$

Now, any two-site reduced density matrix, for arbitrary sites i and j, can be written as

$$\rho_{ij} = \frac{1}{4}(\mathbb{I} + \sum_{\alpha=x,y,z} T_{ij}^{\alpha\alpha} \, \sigma_i^\alpha \otimes \sigma_j^\alpha), \tag{s5}$$

where $\mathbb{I}$ is the two-qubit identity matrix. Since the derivation of the two-site density matrix depends on the diagonalization of $N \times N$ matrices, such as $\mathcal{A}$ and $\mathcal{B}$, the method can be executed for chains with a large number of spins, and allows us to study the asymptotic behavior of several system properties. In our case, these are the long-range quantum correlations.

To obtain the reduced two-site density matrix of the thermal equilibrium state of the quantum spin system, at temperature T, one must find the thermal correlation matrix $\mathcal{G}_{ij}(\beta)$, in a similar fashion to the analytical derivation done above. Here, $\beta = 1/k_B T$, where k_B is the Boltzmann constant. The correlation matrix can be written as

$$\mathcal{G}_{ij}(\beta) = -\sum_k \psi_{ki} \, \phi_{kj} (\langle \eta_k^\dagger \eta_k \rangle_\beta - \langle \eta_k \eta_k^\dagger \rangle_\beta), \tag{s6}$$

where $\eta_k^\dagger$ are the spinless fermionic operators that diagonalize the Hamiltonian, thus generating fermionic excitations in the ground states with energy $|\Delta_k|$. From Fermi statistics, $\langle \eta_k \eta_k^\dagger \rangle_\beta = 1/(\exp[\beta\Delta_k] + 1)$, and hence, $\mathcal{G}_{ij}(\beta) = -\sum_k \psi_{ki} \tanh[\beta\Delta_k/2]\phi_{kj}$. Using $\mathcal{G}_{ij}(\beta)$, the reduced two-site density matrix for the thermal equilibrium state can then be evaluated by following the expressions for the ground state of the spin system as shown in Eqs. (s3 - s4).

S2. MEASURES OF QUANTUM CORRELATION

The correlation functions $T_{ij}^{\alpha\alpha}$ can be used to derive quantum correlation measures, such as quantum discord and entanglement, for reduced two-site density matrices of both the ground and thermal equilibrium states of the system. The obtained two-site reduced density matrix, in Eq. (s5), is Bell-diagonal and hence its quantum discord [S3] can be calculated using an analytical optimization [S4]. For the Bell-diagonal density matrix, ρ_{ij}, its eigenvalues, e_i, can be obtained in terms of $T_{ij}^{\alpha\alpha}$:

$$\begin{aligned} e_1 &= 1/4(1 - T_{ij}^{xx} - T_{ij}^{yy} - T_{ij}^{zz}); \\ e_2 &= 1/4(1 - T_{ij}^{xx} + T_{ij}^{yy} + T_{ij}^{zz}); \\ e_3 &= 1/4(1 + T_{ij}^{xx} - T_{ij}^{yy} + T_{ij}^{zz}); \\ e_4 &= 1/4(1 + T_{ij}^{xx} + T_{ij}^{yy} - T_{ij}^{zz}). \end{aligned} \tag{s7}$$

The quantum mutual information is given by the relation, $\mathcal{I}(\rho_{ij}) = \sum_i e_i \log_2(4e_i)$. The classical correlation obtained after optimization over measurements on a single-party, is given by the relation

$$\mathcal{C}(\rho_{ij}) = \sum_{k=1}^{2} x_k \log_2(2x_k), \quad \text{where} \tag{s8}$$

$$x_k = (1 + (-1)^k x)/2, \quad \text{for } k = (1,2), \quad \text{and} \tag{s9}$$

$$x = \max\{|T_{ij}^{xx}|, |T_{ij}^{yy}|, |T_{ij}^{zz}|\}. \tag{s10}$$

The quantum discord is then given by the relation,

$$\begin{aligned} \mathcal{D}(\rho_{ij}) &= \mathcal{I}(\rho_{ij}) - \mathcal{C}(\rho_{ij}) \\ &= \sum_{i=1}^{4} e_i \log_2(4e_i) - \sum_{k=1}^{2} x_k \log_2(2x_k). \end{aligned} \tag{s11}$$

Similarly, using concurrence [S5] as our measure of choice, the entanglement between any two sites can be analytically derived. Concurrence of a two-qubit density matrix, ρ_{ij}, is defined by the relation

$$\mathcal{E}(\rho_{ij}) = \max\left[0, c_1 - c_2 - c_3 - c_4\right], \tag{s12}$$

where c_i's are the square root of the eigenvalues of the matrix $\rho_{ij}\tilde{\rho_{ij}}$, arranged in decreasing order. $\tilde{\rho_{ij}} = \sigma_i^y \otimes \sigma_j^y \; \rho_{ij}^* \; \sigma_i^y \otimes \sigma_j^y$. For the two-site density matrix obtained in Eq. (s5), $\tilde{\rho_{ij}} = \rho_{ij}$, and c_i's are nothing but the eigenvalues of ρ_{ij}, given by Eq. (s7), arranged in decreasing order. Hence, the concurrence of the obtained two-site reduced density matrix is given by

$$\begin{aligned} \mathcal{E}(\rho_{ij}) &= \max\left[0, 2\, e_{max} - 1\right] \\ &= \max\left[0, \frac{1}{2}(|g_{ij}^+| - h_{ij}^+), \frac{1}{2}(|g_{ij}^-| - h_{ij}^-)\right], \end{aligned} \tag{s13}$$

where $e_{max} = \max[\{e_i\}_{i=1}^4]$, $g_{ij}^\pm = T_{ij}^{xx} \pm T_{ij}^{yy}$, and $h_{ij}^\pm = 1 \pm T_{ij}^{zz}$. Hence, once the correlation functions, $T_{ij}^{\alpha\alpha}$, are known from Eq. (s3), quantum discord and entanglement can be obtained using Eqs. (s13) and (s11), respectively.

To highlight the role of the correlation functions in the behavior of quantum discord and entanglement during the phenomena of adiabatic freezing, we consider an explicit example. Let us study the model considered in the main text: an N-spin open quantum spin chain, with nearest neighbor interactions, with two spins at the edge of the chain (end spins) are weakly coupled to the remaining bulk of $N-2$ spins, as shown in Fig. s1. As presented in the main text, the Hamiltonian for such a spin chain is given by,

$$\mathcal{H} = \mathcal{H}_{bulk} + \mathcal{H}_{end}, \quad \text{where}$$

$$\mathcal{H}_{bulk} = \sum_{i=2}^{N-2} \frac{\kappa}{4} \left(\mathcal{J}_i \, \sigma_i^x \sigma_{i+1}^x + \mathcal{K}_i \, \sigma_i^y \sigma_{i+1}^y\right), \tag{s14}$$

$$\begin{aligned} \mathcal{H}_{end} = \frac{\kappa}{4} \big[&\lambda_1(\sigma_1^x \sigma_2^x + \sigma_{N-1}^x \sigma_N^x) \\ &+ \lambda_2(\sigma_1^y \sigma_2^y + \sigma_{N-1}^y \sigma_N^y)\big]. \end{aligned} \tag{s15}$$

λ_1 and λ_2 are the weak end-couplings, and $\{\mathcal{J}_i\} = \{\mathcal{K}_i\} = 1$, such that the bulk forms an XX spin chain. Adiabatic freezing of long-range quantum correlations is observed, when one of the end-couplings (say, λ_2) is kept fixed, while the other (say, λ_1) is adiabatically varied.

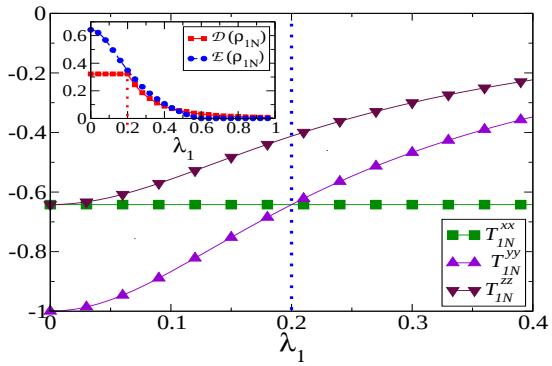

FIG. s2. (Color online.) Variation of long-range two-site correlation functions, T_{1N}^{xx} (green-square), T_{1N}^{yy} (violet-up-triangle), and T_{1N}^{zz} (maroon-down-triangle), with end-coupling strength λ_1, for a spin chain with N = 20. The other end-coupling, λ_2 is kept fixed at 0.2. The inset figure shows the behavior of long-range concurrence (blue-diamond) and quantum discord (square-red). The adiabatic freezing of $\mathcal{D}_L$ for $\lambda_1 \leq \lambda_2$ is evident from the inset figure, whereas entanglement exhibits non-temporal death at λ_1 = 0.59. All quantities used are dimensionless except entanglement (in ebits) and quantum discord (in bits). Compare with Fig. 2 in the main text.

In Fig. s2, one observes the adiabatic freezing of long-range quantum discord ($\mathcal{D}_L$) between the end spins, in the ground

state of the Hamiltonian defined in Eq. (s15), when the end spin coupling satisfies the condition, $\lambda_1 \leq \lambda_2$ (fixed), $\forall\ \lambda_1$. For $\lambda_1 > \lambda_2$ (fixed), $\mathcal{D}_L$ decays with increasing λ_1. This phenomena is however not observed for long-range entanglement ($\mathcal{E}_L$). The behavior of both $\mathcal{D}_L$ and $\mathcal{E}_L$ upon adiabatically varying λ_1 can be explained through the variation of the correlation functions T^{xx}_{1N}, T^{yy}_{1N}, and T^{zz}_{1N} shown in Fig. s2. We observe that $T^{\alpha\alpha}_{1N} < 0$, with $|T^{\alpha\alpha}_{1N}| < 1, \forall\ \alpha = (x, y, z)$, for a spin chain with $N = 20$ spins and λ_2 fixed at 0.2. Since, $T^{zz}_{1N} = -T^{xx}_{1N}\ T^{yy}_{1N}$, therefore T^{xx}_{1N} and T^{yy}_{1N} are the only independent variables, with $|T^{zz}_{1N}| \leq |T^{xx}_{1N}|$ and $|T^{zz}_{1N}| \leq |T^{yy}_{1N}|$. Moreover, T^{xx}_{1N} remains constant with the variation of λ_1.

Consider the region, $\lambda_1 \leq \lambda_2 = 0.2$, in Fig. s2. We see that $|T^{yy}_{1N}| \geq |T^{xx}_{1N}| \geq |T^{zz}_{1N}|$. Therefore, the $\mathcal{C}(\rho_{ij})$ is dependent only on $|T^{yy}_{1N}|$, and decreases with increasing T^{yy}_{1N}. Similarly, $\mathcal{I}(\rho_{ij})$ is varies with $|T^{yy}_{1N}|$ ($|T^{xx}_{1N}|$ is constant) and decreases with an identical rate, thus allowing $\mathcal{D}_L$ to remain frozen for $\lambda_1 \leq \lambda_2 = 0.2$, as observed in the inset of Fig. s2. For $\lambda_1 > \lambda_2 = 0.2$, $|T^{xx}_{1N}| \geq |T^{yy}_{1N}| \geq |T^{zz}_{1N}|$, and $\mathcal{C}(\rho_{ij})$ is dependent only on $|T^{xx}_{1N}|$, which is constant. Therefore, $\mathcal{C}(\rho_{ij})$ is constant for $\lambda_1 > \lambda_2 = 0.2$, but the decreasing $\mathcal{I}(\rho_{ij})$ forces $\mathcal{D}_L$ to decrease, leading to breakdown of freezing. The behavior is consistent with that observed in the phenomena of temporal freezing [S6].

For entanglement, no adiabatic freezing occurs. Since $0 < |T^{\alpha\alpha}_{1N}| < 1, \forall\ \alpha$, the long-range concurrence is given by the relation, $\mathcal{E}_L = \max\left[0, 1/2(|g^+_{1N}| - h^+_{1N})\right]$, where, $|g^+_{1N}| = |T^{xx}_{1N} + T^{yy}_{1N}|$, and $h^+_{1N} = 1 - |T^{xx}_{1N}||\ T^{yy}_{1N}| > 0$. As λ_1 increases $|g^+_{1N}|$ and h^+_{1N} decreases, due to the fact that $|T^{yy}_{1N}|$ decreases, and $T^{xx}_{1N}|$ is constant. For, $|g^+_{1N}| > h^+_{1N}$, $\mathcal{E}_L = 1/2(|g^+_{1N}| - h^+_{1N})$ and decreases with λ_1. For $|g^+_{1N}| \leq h^+_{1N}$, $\mathcal{E}_L = 0$, and long-range entanglement vanishes. The above analysis can be compared with known results on quasi long-range entanglement. For $\lambda_1 = \lambda_2$, the system is isotropic, and we have $T^{xx}_{1N} = T^{yy}_{1N} = z$ (say). Moreover, $T^{zz}_{1N} = -z^2$, which gives us the relation for the long-range entanglement, $\mathcal{E}_L = \max\left[0, 1/2(z^2 + 2|z| - 1))\right]$. Now for $x = -\langle S^x_1 S^x_N + S^y_1 S^y_N\rangle = -1/2\ z$, the above expression for entanglement reduces to $\mathcal{E}_L = 2\max\left[0, (x^2 + |x| - 1/4))\right]$, as shown in [S7].

S3. FREEZING OF ENERGY GAP AND QUANTUM DISCORD, AT LARGE N

An important result discussed in the main text of the letter, is the adiabatic freezing of the energy gap, and its complementary relation to the freezing of quantum discord. In particular, it is shown that for the Hamiltonian in Eq. (s15), the quasi long-range quantum discord between the end spins in the ground state of the system is frozen for $\lambda_1 \leq \lambda_2$, while the energy gap remains constant in the complementary region $\lambda_1 \geq \lambda_2$.

Let us briefly describe the presence of energy gap in the spin Hamiltonian considered in the study. As mentioned in the main text, for the case, $\lambda_1 = \lambda_2 = \lambda$, the dispersion relation of the excitation energy is given by $\Delta_k = \cos(k)$, where k is the quasimomentum modes. These modes satisfy the following

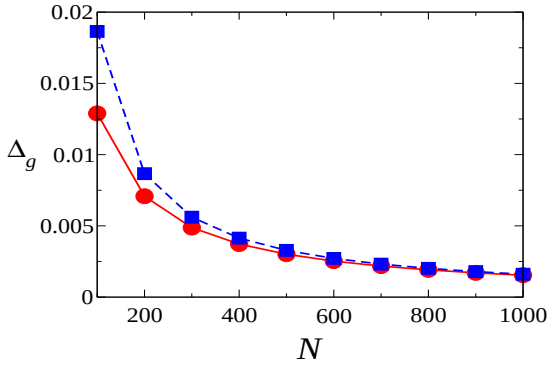

FIG. s3. (Color online.) Variation of the analytically and numerically estimated values of the energy gap with increasing size of the spin chain. The value of energy gap, using the analytical expression, is given by $\Delta_g = \min[f(\lambda_1), f(\lambda_2)]$ (blue-square), where $f(\lambda)$ is defined in Eq. (s16), and for exact numerical calculations (red-circle), for $\lambda_1 = 0.4$ and $\lambda_2 = 0.6$ (and, $\lambda_1 = 0.6$ and $\lambda_2 = 0.4$), for large N. The figure shows that at large N, Δ_g scales linearly as $1/N$.

eigenvalue equation $\cot(k)[\cot((N-1)k/2)] = \lambda^2/(2-\lambda^2)$, for $\lambda \neq 1$, where the positive eigenstate parity has been considered [S7]. The energy gap is then given by k', which minimizes the dispersion relation $\Delta_k = \cos(k')$, while satisfying the above eigenvalue equation.

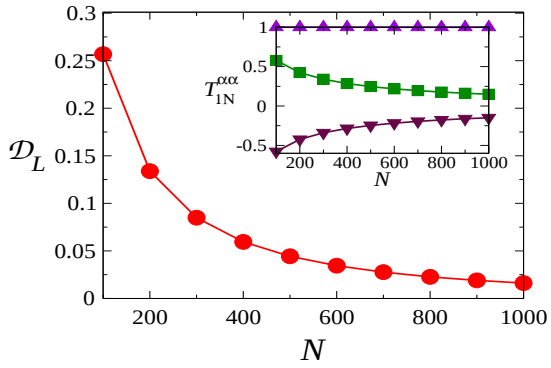

FIG. s4. (Color online.) Variation of the long-range quantum discord (red-circle) with increasing size of the spin chain. The inset shows the behavior of the correlation functions, T^{xx}_{1N} (green-square), T^{zz}_{1N} (maroon-down-triangle), and T^{yy}_{1N} (violet-up-triangle). λ_1 and λ_2 are set at 0.01 and 0.1, respectively. The figure shows that at large N, $\mathcal{D}_L$ scales as $1/N$.

In large N limit, for $k' = \pi/2 - \delta$, where $\delta \to 0$, the dispersion relation provides an analytical expression for the energy gap (Δ_g) as

$$\Delta_g \approx \frac{\pi}{2N}\left(1 + \frac{2}{N(\lambda^2/(2-\lambda^2) + 2}\right) = f(\lambda) \quad \text{(s16)}$$

Numerical analysis for the case, $\lambda_1 \neq \lambda_2$, shows that the quasimomenta k' corresponding to the energy gap satisfies the eigenvalue equation for $\lambda = \min[\lambda_1, \lambda_2]$. Thus, the energy gap is given by the analytical relation, $\Delta_g = \min[f(\lambda_1), f(\lambda_2)]$, where $f(\lambda)$ is defined in Eq. (s16). Figure s3, shows the

agreement between the analytical expression for Δ_g and exact numerical calculations for large N. One can then show that $f(\lambda_1) < f(\lambda_2)$, for $\lambda_1 < \lambda_2$, and $f(\lambda_2) \leq f(\lambda_1)$, for $\lambda_2 \leq \lambda_1$. The adiabatic freezing of the energy gap, as λ_1 is varied, is thus evident for $\lambda_2 \leq \lambda_1$, as Δ_g is independent of λ_1 in this range.

It is known that for the model considered in the study, given by Eq. (s15), the long-range quantum correlation between the end spins is quasi long-range [S7], i.e., the long-range quantum correlation vanishes with increasing N. The behavior of $\mathcal{D}_L$ with increasing system size is shown in Fig. s4, which plots the value of the frozen quantum discord with increasing system size. The figure shows that in the large N limit, both the frozen energy gap and quasi long-range quantum discord scales with $1/N$.

[S1] Lieb E., Schultz T. and Mattis D., *Ann. Phys.*, **16** (1961) 407.

[S2] P. Jordan and E. Wigner, Z. Phys. **47**, 631 (1928).

[S3] Henderson L. and Vedral V., *J. Phys. A*, **34** (2001) 6899; Ollivier H. and Zurek W. H. , Phys. Rev. Lett., **88** (2002) 017901.

[S4] Luo S., *Phys. Rev. A*, **77** 042303 (2008).

[S5] Hill S. and Wootters W. K., *Phys. Rev. Lett.*, **78** (1997) 5022; Wootters W. K., *Phys. Rev. Lett.*, **80** (1998) 2245.

[S6] Mazzola L., Piilo J. and Maniscalco S., *Phys. Rev. Lett.*, **104** (2010) 200401.

[S7] Venuti. L. C. Giampaolo S. M., Illuminati F. and Zanardi P., *Phys. Rev. A*, **76** (2007) 052328.